AGU100 ADVANCING EARTH AND SPACE SCIENCE

Geophysical Research Letters

RESEARCH LETTER
10.1029/2018GL077972

Key Points:
- Iron, cobalt, and vitamin B_{12} amendments were performed in the Equatorial Pacific/Peru upwelling zone at the onset of the 2015 El Niño
- The El Niño Peru upwelling had residual nitrate and exhibited recovery from community-level iron stress following iron amendment
- Mean chlorophyll was enhanced in response to combined iron and cobalt/B_{12} amendment over iron only but was not statistically significant

Supporting Information:
- Supporting Information S1

Correspondence to:
T. J. Browning,
tbrowning@geomar.de

Citation:
Browning, T. J., Rapp, I., Schlosser, C., Gledhill, M., Achterberg, E. P., Bracher, A., & Le Moigne, F. A. C. (2018). Influence of iron, cobalt, and vitamin B_{12} supply on phytoplankton growth in the tropical East Pacific during the 2015 El Niño. *Geophysical Research Letters*, *45*, 6150–6159. https://doi.org/10.1029/2018GL077972

Received 17 MAR 2018
Accepted 4 JUN 2018
Accepted article online 7 JUN 2018
Published online 21 JUN 2018

Influence of Iron, Cobalt, and Vitamin B_{12} Supply on Phytoplankton Growth in the Tropical East Pacific During the 2015 El Niño

Thomas J. Browning[1], Insa Rapp[1], Christian Schlosser[1], Martha Gledhill[1], Eric P. Achterberg[1], Astrid Bracher[2,3], and Frédéric A. C. Le Moigne[1]

[1]Marine Biogeochemistry Division, GEOMAR Helmholtz Centre for Ocean Research, Kiel, Germany, [2]Alfred-Wegener-Institute for Polar and Marine Research, Bremerhaven, Germany, [3]Institute of Environmental Physics, University of Bremen, Bremen, Germany

Abstract Iron (Fe), cobalt (Co), and vitamin B_{12} addition experiments were performed in the eastern Equatorial Pacific/Peruvian upwelling zone during the 2015 El Niño event. Near the Peruvian coastline, apparent photosystem II photochemical efficiencies (F_v/F_m) were unchanged by nutrient addition and chlorophyll *a* tripled in untreated controls over 2 days, indicating nutrient replete conditions. Conversely, Fe amendment further away from the coastline in the high nitrate, low Fe zone significantly increased F_v/F_m and chlorophyll *a* concentrations. Mean chlorophyll *a* was further enhanced following supply of Fe + Co and Fe + B_{12} relative to Fe alone, but this was not statistically significant; further offshore, reported Co depletion relative to Fe could enhance responses. The persistence of Fe limitation in this system under a developing El Niño, as previously demonstrated under non-El Niño conditions, suggests that diminished upwelled Fe is likely an important factor driving reductions in offshore phytoplankton productivity during these events.

Plain Language Summary Phytoplankton productivity in the Equatorial Pacific is critical for curbing CO_2 outgassing from upwelling waters and sustaining globally important fisheries. We tested which micronutrients were limiting phytoplankton growth in the Equatorial Pacific during the 2015 El Niño. To date evidence for nutrient limitation status during these events remains indirect. We show iron is limiting offshore of Peru and that cobalt or vitamin B_{12} could be approaching limitation, with limitation by the latter micronutrients possibly becoming more important further offshore. Linked to satellite data, the new results shed light on critical controls on marine productivity in this biogeochemically/economically important region. Our results suggest reduced upwelled iron-predicted under El Niño conditions would be primarily responsible for observed offshore Peru productivity decreases.

1. Introduction

High levels of phytoplankton productivity in the upwelling regions of the Equatorial Pacific and Peru margin mitigate major CO_2 outgassing (Chavez et al., 1999), lead to emissions of other climate-relevant gases (e.g., Andreae & Raemdonck, 1983; Arevalo-Martínez et al., 2015), and fuel substantial fisheries (e.g., Bakun & Weeks, 2008). The processes regulating phytoplankton growth in these waters are therefore important to resolve. This is particularly pertinent if periodic high magnitude changes in environmental forcing from the El Niño–Southern Oscillation cycle are further modulated by ongoing anthropogenically induced reductions in seawater pH, lowered oxygen concentrations, altered nutrient inputs, and stratification-driven changes in light intensities (Capone & Hutchins, 2013; Chavez et al., 1999).

The potential for Fe-limited growth conditions in this region has been demonstrated by Fe enrichment experiments and via comparison of dissolved Fe concentrations, chlorophyll *a* biomass, phytoplankton fluorescence characteristics, and molecular Fe stress signatures (Bruland et al., 2005; DiTullio et al., 2005; Eldridge et al., 2004; Hutchins et al., 2002; Martin et al., 1994). The possible role of cobalt (Co) in (co-)limiting part of the extant phytoplankton community has also been predicted for this region (Hawco et al., 2016; Saito et al., 2004); furthermore, this has been demonstrated directly in the Costa Rica Dome further to the north (Saito et al., 2005). Co substitutes for zinc (Zn) in carbonic anhydrase in eukaryotic cells (Yee & Morel, 1996), is a metal center in vitamin B_{12} (Morel et al., 2003), and has other probable roles in phosphatases, acyltransferases, and hydratases (e.g., Martinez et al., 2017; Saito et al., 2017). Multiple definitions of "co-limitation" exist (Saito et al., 2008), but it is here tested as a situation where both Fe and Co (or B_{12})

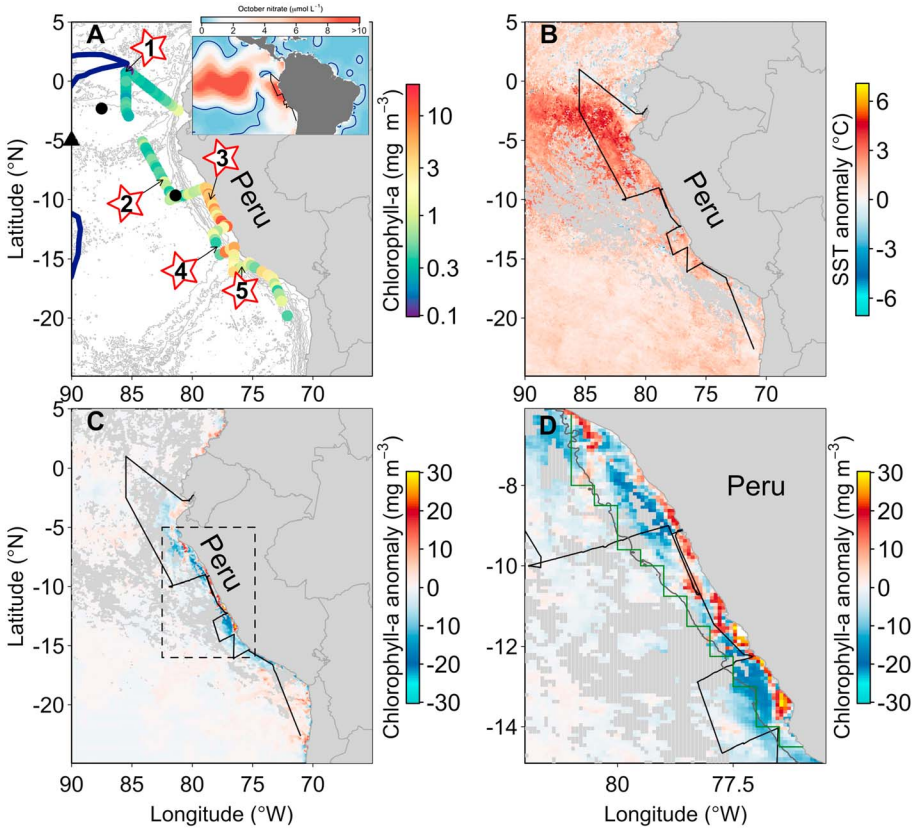

Figure 1. Study region highlighting the biogeochemical setting during occupation. (a) Cruise track showing measured chlorophyll *a* concentrations (colored dots) and incubation experiment locations (numbered stars). The gray contours show bathymetry (1-km depth intervals). The black dots and triangle respectively show the locations of bottle-scale Fe amendment experiments performed by Hutchins et al. (2002) and IronExI reported by Martin et al. (1994). The blue line is the 0.5 μmol L^{-1} climatological World Ocean Atlas nitrate contour for October, displayed for a wider region in the inset map. (b) October 2015 SST anomaly (October 2015 data subtracted from 2002 to 2016 October climatology). (c) As for "b" but for chlorophyll *a* concentration. (d) Boxed region in "c" highlighting Peruvian shelf chlorophyll *a* anomalies. The dark gray line is the 1-km depth contour, and the green line highlights the region used for calculating shelf-averaged chlorophyll *a* anomalies (Figures S1 and S4).

have been simultaneously depleted such that only supplying both in combination results in a statistically significant biomass growth response (Browning et al., 2017). Serial limitation is defined as the sequential biomass enhancement resulting from supplying both the primary (or proximally) limiting nutrient and the next most deficient nutrient (Browning et al., 2017; Moore et al., 2013; Sperfeld et al., 2016).

In an attempt to clarify the potential influences of Fe, Co, and vitamin B_{12} (hereafter referred to simply as B_{12}) on phytoplankton chlorophyll *a* biomass and photophysiological characteristics in Equatorial Pacific and Peru upwelling waters, we conducted five short duration (41–45 hr) Fe, Co, Fe + Co, and supplementary Fe + B_{12} amendment experiments on a research cruise in October 2015. Our experimental testing for limiting nutrients coincided serendipitously with the 2015/2016 El Niño conditions, further allowing us to place our results within the context of physical and chemical anomalies observed on the same research cruise (Stramma et al., 2016) and in the satellite record.

2. Materials and Methods

Experiments were conducted in October 2015 on cruise SO243 (RV *Sonne*; Figure 1). Seawater was collected from a trace-metal-clean towed sampling device at 1–2 m depth linked to a Teflon bellows pump (e.g., Browning et al., 2014, 2017). Mixed layer depths (MLDs) were calculated using water column density derived from conductivity-temperature depth profiles and a 0.125 kg m^{-3} threshold criterion (de Boyer Montégut et al., 2004). Satellite data were downloaded from the NASA ocean color website (https://

oceancolor.gsfc.nasa.gov; all products 9-km resolution reprocessing version R2014.0). Aqua Moderate Resolution Imaging Spectroradiometer (MODIS) chlorophyll *a* concentrations performed better than Visible Infrared Imaging Radiometer Suite (VIIRS) for match-ups with in situ high performance liquid chromatography (HPLC) concentrations (MODIS: $R^2 = 0.83$, RMSE = 0.25; VIIRS: $R^2 = 0.82$, RMSE = 0.43), and data from this sensor were therefore used for further analyses. Temporally overlapping, average chlorophyll *a* concentrations for the Peru shelf were offset between different sensors (see Figure S1 in the supporting information), showing generally much lower values for Sea-viewing Wide Field-of-view Sensor and VIIRS as compared to MODIS. Multivariate El Niño–Southern Oscillation Index (MEI) time series (characterizing El Niño intensity) were downloaded from National Oceanic and Atmospheric Administration (http://www.esrl.noaa.gov/psd/enso/mei/table.html).

Incubation experiments followed a protocol used in several previous expeditions (e.g., Browning et al., 2014, 2017; Ryan-Keogh et al., 2013). Briefly, 18 × 1 L acid-washed polycarbonate bottles were filled following a procedure distributing continuously flowing unfiltered seawater from the trace-metal-clean sampling device across all bottles. Treatment bottles were spiked with 2 nmol L^{-1} Fe, 2 nmol L^{-1} Co, Fe + Co, and Fe + B_{12} (B_{12} concentration of 100 pmol L^{-1}). Fe and Co spikes were made up from 99+ % purity salts in acidified deionized water (Milli-Q, Millipore; $FeCl_3$, ACROS Organics; $CoCl_2$, Carl Roth), and the B_{12} spike solution (Cyanocobalamin; Carl Roth) was passed through a column of a prepared cation exchange resin (Chelex 100) to remove trace metal contamination (Price et al., 1989). Treatments were conducted in triplicate and accompanied by a set of unamended controls. Bottles were incubated in on-deck incubators shaded to ~30% surface irradiance via blue screen filters (Lee filters, type "Blue Lagoon") and maintained at temperatures of surface waters at the time of cruising by continuous flushing from the ship's underway seawater supply system.

Chlorophyll *a* concentrations were determined fluorometrically using a calibrated fluorometer (Turner Designs, Trilogy) after extraction of pigment from GF/F filters (100-mL seawater filtered) in 90% acetone after 12–24 hr in a dark −20 °C freezer (Welschmeyer, 1994). Quantification of extracted phytoplankton pigments (1.1–3.4 L seawater samples filtered onto Whatman GF/F filters, flash frozen, and stored at −80 °C) was performed via HPLC following Barlow et al. (1997) with modifications described in Taylor et al. (2011). Phytoplankton groups were derived from phytoplankton pigments as described in Booge et al. (2018).

Phytoplankton photophysiological measurements were performed using a FASTOcean Fast Repetition Rate fluorometer in bench top mode with an integrated FASTact laboratory system (Chelsea Technologies Ltd). Single acquisitions were performed using 100 × 1 μs blue excitation flashes, and data were fit using the model of Kolber et al. (1998) within the manufacturer's software (FASTPro8). Blanks (0.2-μm syringe-filtered samples) were typically run for one replicate per treatment, and blank fluorescence was subtracted from F_o and F_m before calculation of $F_v/F_m = (F_m - F_o)/F_m$.

Seawater samples for dissolved trace element analysis were collected in acid-washed 125-mL low-density polyethylene sample bottles (Nalgene), filtered inline using a 0.8/0.2-μm AcroPak1000™ (Pall) filter capsule. Samples were acidified with ultrapure hydrochloric acid (UpA grade, Romil) to pH 1.9 for >6 months, subject to 4-hr UV irradiation in 30-mL fluorinated ethylene propylene bottles, preconcentrated on a modified Sea*FAST* system (Elemental Scientific Inc), and then analyzed using an Element XR inductively coupled plasma-mass spectrometer (Thermo Finnigan; Rapp et al., 2017). Isotope dilution and standard additions were used to quantify Fe and Co, respectively. Manifold and buffer blanks were determined and subtracted from analyzed concentrations as described in Rapp et al. (2017)—Fe buffer blank: 0.024 nmol L^{-1} + manifold blank: 0.0334 ± 0.0044 nmol L^{-1} (n = 17); Co buffer blank: 0.001 nmol L^{-1} + manifold blank: 0.0021 ± 0.0007 nmol L^{-1} (n = 17). Analyzed concentrations were validated via good agreement with certified reference material (Table S1 in the supporting information). Macronutrient samples were analyzed on-ship using a QuAAtro autoanalyzer (Seal Analytical), as described by Stramma et al. (2016).

3. Results and Discussion

3.1. Initial Conditions

Cruise dates were at the onset of the 2015/2016 El Niño: MEI was near the maximum observed for this event (October 2015 MEI = 2.3 cf. event maximum in August 2015 = 2.5), with positive surface temperature

Table 1
Starting Conditions for Bioassay Experiments

	Experiment number				
	1	2	3	4	5
	Eq. Pacific	Off-shelf Peru	On-shelf Peru	Off-shelf Peru	Midshelf Peru
Longitude (°W)	85.49	82.42	78.50	77.94	75.89
Latitude (°N)	0.82	−8.34	−9.97	−13.10	−15.67
Coast distance (km)	420	266	26	143	73
SST (°C)	26.2	22.3	17.8	18.2	18.0
SST variability (°C)[a]	3.2	2.4	3.2	2.9	4.1
MLD (m)	21.0	~20[b]	~13[b]	33.8	24.5
$NO_2 + NO_3$ (μmol L^{-1})	0.06	7.46	20.33	26.02	9.67
PO_4 (μmol L^{-1})	0.20	1.02	1.79	2.18	1.31
SiO_2 (μmol L^{-1})	1.09	3.34	14.14	16.13	6.15
dFe (nmol L^{-1})	0.06	0.13	2.22	0.31	0.68
dCo (nmol L^{-1})	0.021	0.041	0.086	0.13	0.11
Fe_N* (nmol L^{-1})	0.036	−2.86	−5.93	−10.12	−3.20
Co_{Fe}* (nmol L^{-1})	0.019	0.038	0.030	0.122	0.093
Chl *a* (mg m^{-3})	0.20	0.33	4.26	1.45	1.62
F_v/F_m	0.30	0.31	0.47	0.37	0.44
Dominant accessory pigments	Zea> 19′Hex> 19′But	Fuco> 19′Hex> Chl c1 + c2	Fuco> Chl *b*> Chl c1 + c2	19′Hex> Chl *b*> 19′But	Chl *b*> 19′But> 19′Hex
Dominant phytoplankton	Cyanobacteria, Haptophytes	Diatoms, Haptophytes	Diatoms, Chlorophytes	Haptophytes, Chlorophytes	Chlorophytes, Haptophytes

Note. Fe_N* and Co_{Fe}* are Fe and Co concentrations in excess of assumed-average phytoplankton requirements relative to nitrate and Fe, respectively.
$Fe_N^* = Fe - (NO_2 + NO_3)\ R_{Fe:N}$.
$Co_{Fe}^* = Co - Fe\ R_{Co:Fe}$.
Where $R_{Fe:N}$ and $R_{Co:Fe}$ are assumed-average Fe:N (0.469×10^{-3} mol:mol) and Co:Fe (0.025 mol: mol) stoichiometry in phytoplankton (Moore et al., 2013). After Parekh et al. (2005) and Ito et al. (2005).
Zea = zeaxanthin; 19′Hex = 19′-hexanoyloxyfucoxanthin; 19′But = 19′-butanoyloxyfucoxanthin; Fuco = fucoxanthin.
[a]Maximum variability in underway SST over the time course of the incubation. [b]Calculated from nearest conductivity-temperature depth station profile.

anomalies throughout the cruise region (Figure 1b; Stramma et al., 2016). Bioassay experiments were conducted in three distinct oceanographic regimes (Figures 1, S2, and S3 and Table 1): (i) experiment 1: warm (26.2 °C) equatorial waters with depleted nitrate (0.06 μmol L^{-1}), 21 m MLD, and a relatively low chlorophyll *a* concentration (0.20 mg m^{-3}), with diagnostic pigments suggesting dominance of cyanobacteria (both *Prochlorococcus* and *Synechococcus*) and haptophytes; (ii) experiments 2, 4, and 5: cooler Humboldt Current waters (18.0–22.3 °C) with residual nitrate (7.46–26.0 μmol L^{-1}), MLDs ~20–33.8 m, and elevated chlorophyll *a* (0.33–1.62 mg m^{-3}) and diagnostic pigments suggesting dominance of diatoms, haptophytes, and chlorophytes; (iii) experiment 3: Peruvian shelf waters with elevated nitrate concentrations (20.3 μmol L^{-1}), shoaled MLDs (~13 m), and an enhanced chlorophyll *a* concentration (4.26 mg m^{-3}) with diagnostic pigments suggesting dominance of diatoms and chlorophytes.

3.2. Spatial Patterns of Fe Limitation

Fe stress at experimental sites was evaluated via F_v/F_m changes following incubation of seawater with added Fe, with increases interpreted to reflect coupling of energetically "detached" light harvesting complexes with PSII reaction centers (Behrenfeld & Milligan, 2013; Macey et al., 2014). Associated increases in chlorophyll *a* were interpreted as representing proximal limitation of biomass accumulation by Fe availability. Micronutrient amendment in experiment 1 resulted in no statistically significant F_v/F_m or chlorophyll *a* increases over control bottles (Figures 2a and 2f), suggesting that the community was not proximally Fe/Co/B_{12} stressed/limited (Browning et al., 2014, 2017; Ryan-Keogh et al., 2013). This contrasts with previous experiments conducted nearby. Both Martin et al. (1994) and Hutchins et al. (2002) reported proximal Fe limitation of phytoplankton communities at nearby locations (Figure 1a) in the same season (September–October), and Saito et al. (2005) found Fe-Co co-limitation further to the north in the Costa Rica upwelling dome. In all three previous studies residual nitrate was present (~3.5–10.8 μmol L^{-1}), whereas at our experimental site nitrate was depleted (0.06 μmol L^{-1}; Table 1), which suggested that the site was

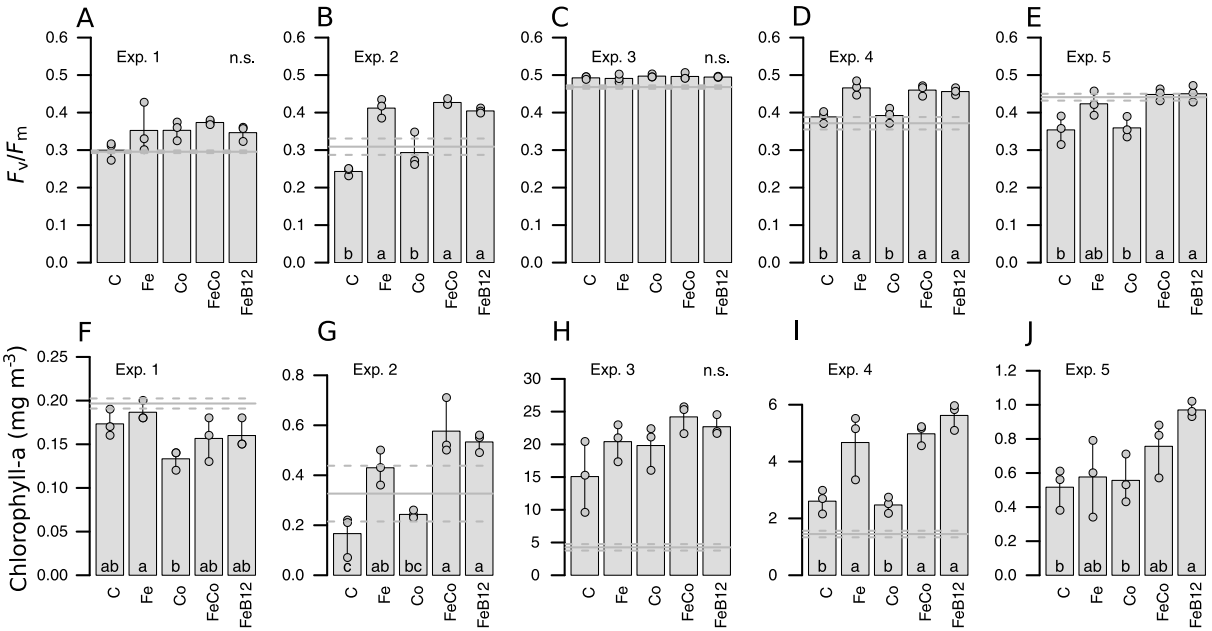

Figure 2. Phytoplankton responses to nutrient amendment. (a–e) F_v/F_m and (f–j) chlorophyll *a* biomass changes bioassay experiments. The bar heights indicate means (n = 3); the dots show individual bottle replicates and lines indicate the range (n = 3). The letters show the results of a test for statistically significant different means (ANOVA $p < 0.05$ followed by a Tukey honesty significant difference test): The bars labeled with the same letter are statistically indistinguishable and n. s. = not significant. The gray horizontal lines indicate initial conditions (dashed lines = range; solid lines = mean). The mean starting chlorophyll *a* in experiment 5 was 1.62 mg m^{-3}.

proximally N-limited or possibly N-Fe co-limited (Behrenfeld et al., 2006; Browning et al., 2017; DiTullio et al., 1993; Saito et al., 2014).

Although the prevalent El Niño conditions appeared to induce near-cessation of the Equatorial Undercurrent upwelling (Stramma et al., 2016), which could be hypothesized to have reduced supply rates of waters with low Fe:N ratios to the site of experiment 1, nitrate concentrations at this site from the World Ocean Atlas climatology show depletion to <2.9 μmol L^{-1} from July to January (0.76 μmol L^{-1} in October). Surface seawaters in these months are warmer and fresher, with an altered surface ocean current direction (Figure S3). Therefore, while nitrate depletion was slightly accentuated beyond climatological averages during our El Niño occupation, observed differences in responses to Fe amendment in our experiment 1 and previous studies probably originate primarily from relatively subtle geographic position within the strong regional nitrate gradient (Figures 1a inset and S3; Hutchins et al., 2002; Martin et al., 1994).

The one experiment conducted near the Peruvian coastline (experiment 3; Figures 2c and 2h) showed no significant F_v/F_m or chlorophyll *a* response to Fe amendment relative to controls (alone or in combination with Co/B_{12}). This suggested that Fe availability was neither stressing the initial phytoplankton community nor limiting chlorophyll *a* biomass accumulation. This was consistent with the relatively high dissolved Fe concentrations measured in initial experimental seawater (2.22 nmol L^{-1}). Although statistically insignificant, mean chlorophyll *a* for all Fe amended combinations at this site were enhanced relative to non-Fe treatments (control, +Co). This could suggest the substantial growth that occurred across all incubated bottles led to significant Fe drawdown, with the supplementary Fe supply enabling additional growth. However, F_v/F_m in non-Fe treatments remained high, arguing against such an interpretation.

In contrast, Fe amendment—alone or in combination with Co or B_{12}—in experiments located further offshore (experiments 2, 4, and 5) led to significant F_v/F_m increases relative to control and Co-amended bottles (Figure 2). Significant increases in chlorophyll *a* concentrations were also observed for all Fe-amended combinations in experiments 2 and 4. In experiment 5, although Fe stress was evident in the control and +Co bottles (i.e., having significantly lower F_v/F_m than Fe amended combinations), both F_v/F_m and chlorophyll *a* declined from initial values, possibly caused by high levels of grazing and/or significant photoacclimation during the incubation (e.g., Behrenfeld & Milligan, 2013). Regardless of the latter, experiments 2–5

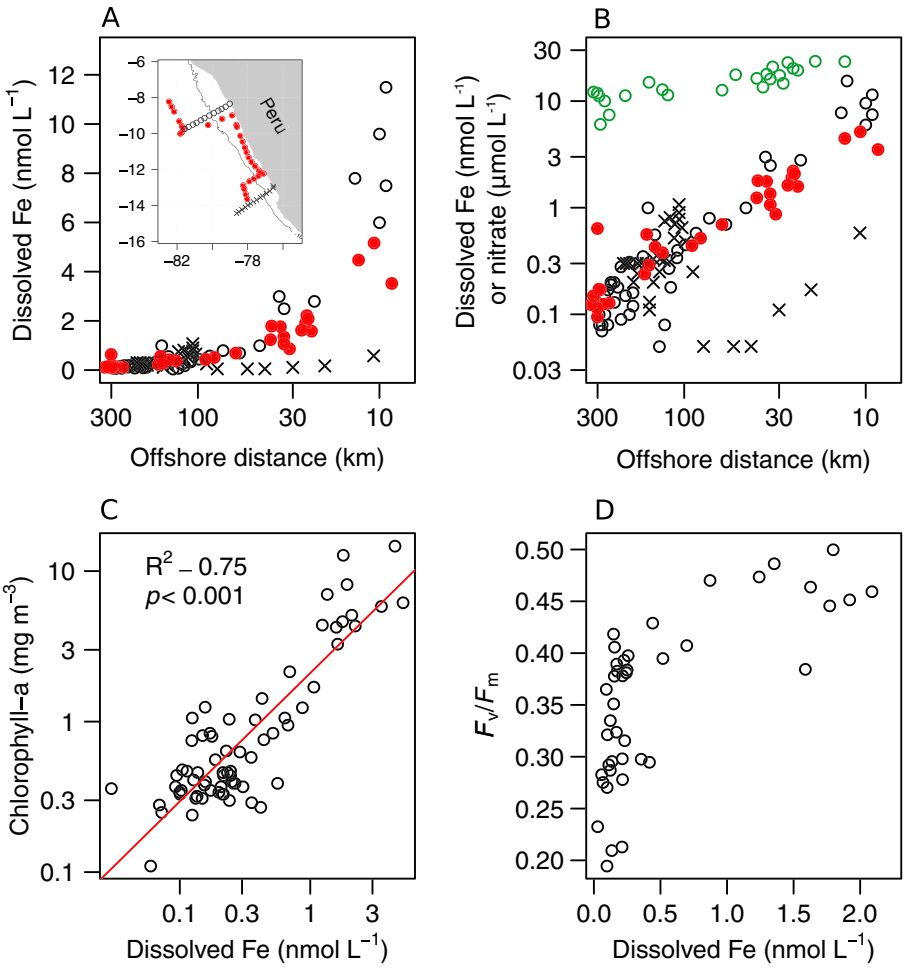

Figure 3. Potential impact of Fe availability on phytoplankton. (a) Offshore decline in surface dissolved Fe concentrations (note logarithmic distance scaling). The red dots are data from this study (locations highlighted in inset map), and the black symbols are data from Bruland et al. (2005) (from Tagliabue et al., 2012 data set) for two transects that ran perpendicular to the coast. Shelf width is highlighted by the 1-km depth contour on the inset map. The southern cross-shelf transect of Bruland et al. (2005) had lower Fe concentrations (crosses) than more northerly transects in both studies, probably resulting from a narrower shelf width for sedimentary Fe entrainment into upwelled waters (Bruland et al., 2005). (b) Same as "a" but with dissolved Fe on a logarithmic scale. Surface nitrate concentrations from this study (same sampling locations as "a") are plotted in green. (c) Correlation of log-transformed dissolved Fe and chlorophyll *a* biomass (note for linear correlation: $R^2 = 0.67$, $p < 0.001$). (d) Dissolved Fe and F_v/F_m.

collectively confirmed reductions in dissolved Fe in the transition offshore from the Peruvian coastline (Figures 3a and 3b) as being a key driver for matching declines in chlorophyll *a* (Figures 1a and 3c) and nighttime F_v/F_m (Figure 3d), both measured in this study and previously under non-El Niño conditions by Bruland et al. (2005).

3.3. Potential Role for Co/Vitamin B_{12} in Coregulating Phytoplankton Yield in the Equatorial Pacific

Some limited evidence was found for Co and/or B_{12} becoming serially limiting at the community level in the Peru upwelling following supply of Fe. For all experiments conducted in waters with elevated nitrate (experiments 2–5), the mean chlorophyll *a* response following amendment with Fe + Co or Fe + B_{12} was always higher than that following amendment with Fe or Co alone (Figures 2g–2j). These responses were, however, not statistically resolvable, either within individual experiments (Figure 2) or when normalized chlorophyll *a* responses were aggregated across all experiments (not shown). Therefore, while mean changes at individual sites could be interpreted to suggest the potential for serial Co/B_{12} limitation, such conditions were not fully established in these waters (cf. Bertrand et al., 2007; Browning et al., 2017; Saito et al., 2005).

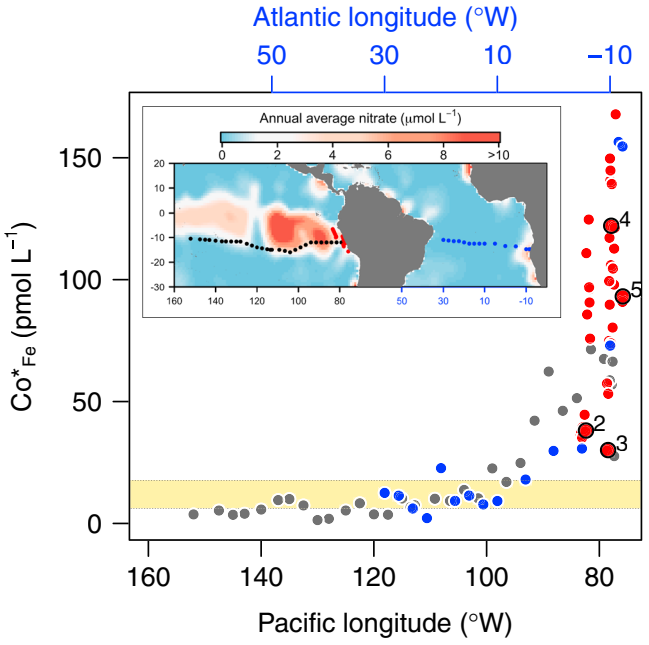

Figure 4. Potential for co-serial/co-limitation offshore of the Peru upwelling. The vertical axis is Co_{Fe}*, the "excess" dissolved Co concentration relative to Fe assuming average phytoplankton requirements (see Table 1). The red dots indicate Co_{Fe}* for the Peru upwelling region (this study), with initial values for the four bottle incubation experiments in this zone labeled. The black and blue data points represent surface waters (<10 m depth) of the GEOTRACES GP16 and GAc01 cruises, respectively (Hawco et al., 2016; Noble et al., 2012; Resing et al., 2015). The yellow shading highlights the Co_{Fe}* range at experimental sites exhibiting significant serial co-limitation in the SE Atlantic (Browning et al., 2017). Note the Atlantic-Pacific cruises were at similar latitudes and that the two ocean basins represented in the figure have longitude scales that differ but are of the same absolute magnitude.

This may not have been the case if sites had been occupied further offshore (Figure 4). Calculations using available GEOTRACES data show continued Co loss from surface waters, relative to Fe, with distance offshore from Peru. Eventually, the biological "excess" of Co over Fe becomes less than SE Atlantic experimental sites where clear serial responses to Co addition have been observed previously (Figure 4; Browning et al., 2017; Hawco et al., 2016; Resing et al., 2015). Acknowledging the potential for changes in community-level Co/B_{12} demand and bioavailability, this enhanced loss of Co offshore from Peru could be hypothesized to result in similar observations of widespread serial or co-limitation by Co in the Equatorial Pacific (Bertrand et al., 2007, 2011, 2015; Heal et al., 2017; Helliwell et al., 2015, 2016; Panzeca et al., 2008; Saito et al., 2004, 2005; Sañudo-Wilhelmy et al., 2012).

3.4. Potential Impact of El Niño Conditions on Chlorophyll *a*

The isopycnal and macronutrient distribution in October 2015 suggested active wind-driven upwelling along the Peruvian shelf—despite El Niño status—but was dominated by warmer, more oxygenated waters than non-El Niño conditions (Stramma et al., 2016). Discrete sampling within the on-shelf, near coastal zone revealed high surface nitrate (13.6–23.6 μmol L^{-1}) and relatively high chlorophyll *a* (up to 14.7 mg m^{-3} measured), as found during non-El Niño conditions (Bruland et al., 2005; DiTullio et al., 2005).

Area-averaged, on-shelf satellite-derived chlorophyll *a* for October 2015 was similar to a 2002–2016 climatology (Figures S1 and S4). However, there was a geographic redistribution of temporally averaged concentrations over the shelf, with positive anomalies (higher chlorophyll concentrations) in the near-coastal zone and negative anomalies (lower chlorophyll concentrations) further offshore toward the 1-km water depth contour (Figures 1c and 1d). Geographically patchy, high magnitude chlorophyll *a* anomalies in this region are common in the satellite record and not uniquely associated with El Niño events (Figure S5). The one experiment conducted in the near-coastal zone (experiment 3) led to chlorophyll *a* accumulation in all incubated experimental bottles, including unamended controls (e.g., mean average of 3.5 × chlorophyll *a* increases in control bottles over initial concentrations). This suggested that these near-coastal seawaters, in addition to having sufficient macronutrients, were also $Fe/Co/B_{12}$-replete, with experimental confinement potentially resulting in (i) relief of light limitation and/or (ii) isolation from grazing and/or (iii) prohibited dilution/dispersal, which subsequently allowed chlorophyll *a* to accumulate (e.g., Cullen et al., 1992; Moore et al., 2006). Given (micro) nutrient concentrations under non-El Niño conditions in this near-coastal regime are also elevated (Bruland et al., 2005), such factors (i.e., enhanced light and reduced phytoplankton loss) could be hypothesized to have contributed to the positive satellite chlorophyll *a* anomalies observed (Figures 1c and 1d).

In contrast to near-coastal waters, experiments and across-shelf observations demonstrated a rapid offshore transition to Fe limited conditions (experiments 2–5; Figure 2). Changes in Fe supply offshore could therefore be an important factor regulating phytoplankton productivity in these waters (Bruland et al., 2005; Johnson et al., 1999), potentially resulting in the generally negative surface chlorophyll *a* anomalies recorded by satellite away from the Peru coastline during our occupation (Figure 3d). Although it is difficult to compare the surface-most (1–2 m depth) Fe concentrations presented here with those collected under non-El Niño conditions in the context of Fe delivery to the euphotic zone (Figures 3a and 3b; Bruland et al., 2005), several factors can be hypothesized to have reduced bioavailable Fe supply under the atypical El Niño conditions characterizing our cruise occupation. First, the upwelling of warmer, more oxygenated waters over the northern Peruvian shelf during our occupation may have reduced sedimentary Fe efflux and water column retention (Bruland et al., 2005; Johnson et al., 1999; Liu & Millero, 2002; Lohan & Bruland, 2008; Scholz et al., 2016; Stramma et al., 2016). Second, warmer and more oxygenated seawaters may have reduced the

solubility of inorganic Fe (III) species (Schlosser et al., 2012) and/or the fraction of dissolved Fe in the form of more bioavailable Fe (II) species (Liu & Millero, 2002; Shaked & Lis, 2012). Third, the formation and sinking of more biogenic particles in higher chlorophyll *a* waters nearest the Peru coast would have removed more Fe from the dissolved pool, leaving less Fe to be advected offshore (Figure 1d).

4. Conclusions

Following earlier studies testing for Fe limitation in the Equatorial Pacific (Bruland et al., 2005; Eldridge et al., 2004; Hutchins et al., 2002; Martin et al., 1994), five new bioassay experiments have confirmed a patchwork of community-level Fe limitation dictated by proximity to high-Fe coastal waters and position within the regional nitrate gradient. Our results suggest that any reduction in offshore supply of bioavailable Fe could play a central role in reducing phytoplankton yields in proximity to the Peruvian shelf under El Niño conditions (Figure 3; Barber and Chávez, 1986; Espinoza-Morriberón et al., 2017). However, alongside Fe availability, the net effect of several environmental drivers affecting multiple trophic levels might be needed to resolve the mechanisms underpinning chlorophyll *a* changes (Behrenfeld & Boss, 2014; Boyd et al., 2014; Chen et al., 2012; Jackson et al., 2011; Mackas et al., 1985; Ulloa et al., 2001).

Evidence for Co and/or B_{12} becoming serially limiting following Fe supply was confined to statistically insignificant mean chlorophyll *a* enhancements following Fe + Co/B_{12} addition relative to Fe alone. Alterations in Fe:Co supply ratios to surface waters, for example, due to divergent metal source strengths (e.g., via modified aerosol or sediment supply), solubility controls (e.g., seawater oxidation state, temperature, and ligand types/concentrations), and removal process (e.g., precipitation, scavenging, and phytoplankton elemental stoichiometry), could regulate whether Co/B_{12} (co-/serial) limitation ever occurs in the Peru upwelling (Browning et al., 2017; Hawco et al., 2016; King et al., 2011; Koch et al., 2011; Saito et al., 2004, 2005). Further offshore from the Peru coastline, open ocean GEOTRACES data show continued Co loss relative to Fe in surface seawater, indicating that Co/B_{12} co-/serial limitation could be at least as prevalent as that recently discovered in the SE Atlantic (Browning et al., 2017), potentially playing a role in restricting phytoplankton growth and full nitrate drawdown following an excess supply of Fe (Martin et al., 1994).

Acknowledgments
We thank the captain, crew, and principle scientists (C. Marandino, T. Steinhoff, and D. Grundle) of the RV *Sonne SO243* cruise. M. Lohmann is thanked for performing the nutrient measurements, S. Wiegmann for HPLC pigment analyses, R. Röttgers for assistance with pigment sampling and discussion, and M. Lomas for useful discussion. N. Hawco and an anonymous reviewer are thanked for comments that significantly improved an earlier version of this manuscript. The research cruise was funded by the Bundesministerium für Bildung und Forschung (03G0243A). T.J.B. was funded by a Marie Skłodowska-Curie Postdoctoral European Fellowship (OceanLiNES; grant 658035). Data from this manuscript are available from PANGAEA (https://doi.pangaea.de/10.1594/PANGAEA.890130) and the NASA Ocean Color website (https://oceancolor.gsfc.nasa.gov).

References

Andreae, M. O., & Raemdonck, H. (1983). Dimethyl sulfide in the surface ocean and the marine atmosphere: A global view. *Science*, *221*(4612), 744–747. https://doi.org/10.1126/science.221.4612.744

Arevalo-Martínez, D. L., Kock, A., Löscher, C. R., Schmitz, R. A., & Bange, H. W. (2015). Massive nitrous oxide emissions from the tropical South Pacific Ocean. *Nature Geoscience*, *8*(7), 530–533. https://doi.org/10.1038/ngeo2469

Bakun, A., & Weeks, S. J. (2008). The marine ecosystem off Peru: What are the secrets of its fishery productivity and what might its future hold? *Progress in Oceanography*, *79*(2–4), 290–299. https://doi.org/10.1016/j.pocean.2008.10.027

Barber, R. T., & Chávez, F. P. (1986). Ocean variability in relation to living resources during the 1982–83 El Niño. *Nature*, *319*(6051), 279–285. https://doi.org/10.1038/319279a0

Barlow, R. G., Cummings, D. G., & Gibb, S. W. (1997). Improved resolution of mono- and divinyl chlorophylls a and b and zeaxanthin and lutein in phytoplankton extracts using reverse phase C-8 HPLC. *Marine Ecology Progress Series*, *161*, 303–307. https://doi.org/10.3354/meps161303

Behrenfeld, M. J., & Boss, E. S. (2014). Resurrecting the ecological underpinnings of ocean plankton blooms. *Annual Review of Marine Science*, *6*(1), 167–194. https://doi.org/10.1146/annurev-marine-052913-021325

Behrenfeld, M. J., & Milligan, A. J. (2013). Photophysiological expressions of iron stress in phytoplankton. *Annual Review of Marine Science*, *5*(1), 217–246. https://doi.org/10.1146/annurev-marine-121211-172356

Behrenfeld, M. J., Worthington, K., Sherrell, R. M., Chavez, F. P., Strutton, P., McPhaden, M., & Shea, D. M. (2006). Controls on tropical Pacific Ocean productivity revealed through nutrient stress diagnostics. *Nature*, *442*(7106), 1025–1028. https://doi.org/10.1038/nature05083

Bertrand, E. M., McCrow, J. P., Moustafa, A., Zheng, H., McQuaid, J. B., Delmont, T. O., et al. (2015). Phytoplankton-bacterial interactions mediate micronutrient colimitation at the coastal Antarctic Sea ice edge. *Proceedings of the National Academy of Sciences of the United States of America*, *112*(32), 9938–9943. https://doi.org/10.1073/pnas.1501615112

Bertrand, E. M., Saito, M. A., Lee, P. A., Dunbar, R. B., Sedwick, P. N., & DiTullio, G. R. (2011). Iron limitation of a springtime bacterial and phytoplankton community in the Ross Sea: Implications for vitamin B12 nutrition. *Frontiers in Microbiology*, *2*, 1–12. https://doi.org/10.3389/fmicb.2011.00160

Bertrand, E. M., Saito, M. A., Rose, J. M., Riesselman, C. R., Lohan, M. C., Noble, A. E., et al. (2007). Vitamin B12 and iron colimitation of phytoplankton growth in the Ross Sea. *Limnology and Oceanography*, *52*(3), 1079–1093. https://doi.org/10.4319/lo.2007.52.3.1079

Booge, D., Schlundt, C., Bracher, A., Endres, S., Zäncker, B., & Marandino, C. A. (2018). Marine isoprene production and consumption in the mixed layer of the surface ocean—A field study over 2 oceanic regions. *Biogeosciences*, *15*(2), 649–667. https://doi.org/10.5194/bg-15-649-2018

Boyd, P. W., Lennartz, S. T., Glover, D. M., & Doney, S. C. (2014). Biological ramifications of climate-change-mediated oceanic multi-stressors. *Nature Climate Change*, *5*(1), 71–79. https://doi.org/10.1038/nclimate2441

Browning, T. J., Achterberg, E. P., Rapp, I., Engel, A., Bertrand, E. M., Tagliabue, A., & Moore, C. M. (2017). Nutrient co-limitation at the boundary of an oceanic gyre. *Nature*, *551*, 242–246. https://doi.org/10.1038/nature24063

Browning, T. J., Bouman, H. A., Moore, C. M., Schlosser, C., Tarran, G. A., Woodward, E. M. S., & Henderson, G. M. (2014). Nutrient regimes control phytoplankton ecophysiology in the South Atlantic. *Biogeosciences*, *11*(2), 463–479. https://doi.org/10.5194/bg-11-463-2014

Bruland, K. W., Rue, E. L., Smith, G. J., & DiTullio, G. R. (2005). Iron, macronutrients and diatom blooms in the Peru upwelling regime: Brown and blue waters of Peru. *Marine Chemistry*, *93*(2–4), 81–103. https://doi.org/10.1016/j.marchem.2004.06.011

Capone, D. G., & Hutchins, D. A. (2013). Microbial biogeochemistry of coastal upwelling regimes in a changing ocean. *Nature Geoscience*, *6*(9), 711–717. https://doi.org/10.1038/ngeo1916

Chavez, F. P., Strutton, P. G., Friederich, G. E., Feely, R. A., Feldman, G. C., Foley, D. G., & Mcphaden, M. J. (1999). Biological and chemical response of the equatorial pacific ocean to the 1997–98 El Nino. *Science*, *286*(5447), 2126–2131. https://doi.org/10.1126/science.286.5447.2126

Chen, B., Landry, M. R., Huang, B., & Liu, H. (2012). Does warming enhance the effect of microzooplankton grazing on marine phytoplankton in the ocean? *Limnology and Oceanography*, *57*(2), 519–526. https://doi.org/10.4319/lo.2012.57.2.0519

Cullen, J. J., Yang, X., & MacIntyre, H. L. (1992). Nutrient limitation of marine photosynthesis. *Primary Productivity and Biogeochemical Cycles in the Sea*, 69–88. https://doi.org/10.1007/978-1-4899-0762-2_5

de Boyer Montégut, C., Madec, G., Fischer, A. S., Lazar, A., & Ludicone, D. (2004). Mixed layer depth over the global ocean: An examination of profile data and a profile-based climatology. *Journal of Geophysical Research*, *109*, C12003. https://doi.org/10.1029/2004JC002378

DiTullio, G. R., Geesey, M. E., Maucher, J. M., Alm, M. B., Riseman, S. F., & Bruland, K. W. (2005). Influence of iron on algal community composition and physiological status in the Peru upwelling system. *Limnology and Oceanography*, *50*(6), 1887–1907. https://doi.org/10.4319/lo.2005.50.6.1887

DiTullio, G. R., Hutchins, D. A., & Bruland, K. W. (1993). Interaction of iron and major nutrients controls phytoplankton growth and species composition in the tropical North Pacific Ocean. *Limnology and Oceanography*, *38*(3), 495–508. https://doi.org/10.4319/lo.1993.38.3.0495

Eldridge, M. L., Trick, C. G., Alm, M., DiTullio, G. R., Rue, E. L., Bruland, K. W., et al. (2004). Phytoplankton community response to a manipulation of bioavailable iron in HNLC waters of the subtropical Pacific Ocean. *Aquatic Microbial Ecology*, *35*(1), 79–91. https://doi.org/10.3354/ame035079

Espinoza-Morriberón, D., Echevin, V., Colas, F., Tam, J., Ledesma, J., Vásquez, L., & Graco, M. (2017). Impacts of El Niño events on the Peruvian upwelling system productivity. *Journal of Geophysical Research: Oceans*, *122*, 5423–5444. https://doi.org/10.1002/2016JC012439

Hawco, N. J., Ohnemus, D. C., Resing, J. A., Twining, B. S., & Saito, M. A. (2016). A cobalt plume in the oxygen minimum zone of the eastern tropical South Pacific. *Biogeosciences*, 1–60. https://doi.org/10.5194/bg-2016-169

Heal, K. R., Qin, W., Ribalet, F., Bertagnolli, A. D., Coyote-Maestas, W., Hmelo, L. R., et al. (2017). Two distinct pools of B12 analogs reveal community interdependencies in the ocean. *Proceedings of the National Academy of Sciences of the United States of America*, *114*(2), 364–369. https://doi.org/10.1073/pnas.1608462114

Helliwell, K. E., Collins, S., Kazamia, E., Purton, S., Wheeler, G. L., & Smith, A. G. (2015). Fundamental shift in vitamin B12 eco-physiology of a model alga demonstrated by experimental evolution. *The ISME Journal*, *9*(6), 1446–1455. https://doi.org/10.1038/ismej.2014.230

Helliwell, K. E., Lawrence, A. D., Holzer, A., Kudahl, U. J., Sasso, S., Kräutler, B., et al. (2016). Cyanobacteria and eukaryotic algae use different chemical variants of vitamin B12. *Current Biology*, *26*(8), 999–1008. https://doi.org/10.1016/j.cub.2016.02.041

Hutchins, D. A., Hare, C. E., Weaver, R. S., Zhang, Y., Firme, G. F., DiTullio, G. R., et al. (2002). Phytoplankton iron limitation in the Humboldt Current and Peru upwelling. *Limnology and Oceanography*, *47*(4), 997–1011. https://doi.org/10.4319/lo.2002.47.4.0997

Ito, T., Parekh, P., Dutkiewicz, S., & Follows, M. J. (2005). The Antarctic circumpolar productivity belt. *Geophysical Research Letters*, *32*, L13604. https://doi.org/10.1029/2005GL023021

Jackson, T., Bouman, H. A., Sathyendranath, S., & Devred, E. (2011). Regional-scale changes in diatom distribution in the Humboldt upwelling system as revealed by remote sensing: Implications for fisheries. *ICES Journal of Marine Science*, *68*(4), 729–736. https://doi.org/10.1093/icesjms/fsq181

Johnson, K. S., Chavez, F. P., & Friederich, G. E. (1999). Continental-shelf sediment as a primary source of iron for coastal phytoplankton. *Nature*, *398*(6729), 697–700. https://doi.org/10.1038/19511

King, A. L., Sañudo-Wilhelmy, S. A., Leblanc, K., Hutchins, D. A., & Fu, F. (2011). CO2 and vitamin B12 interactions determine bioactive trace metal requirements of a subarctic Pacific diatom. *The ISME Journal*, *5*(8), 1388–1396. https://doi.org/10.1038/ismej.2010.211

Koch, F., Alejandra Marcoval, M., Panzeca, C., Bruland, K. W., Sañudo-Wilhelmy, S. A., & Gobler, C. J. (2011). The effect of vitamin B12 on phytoplankton growth and community structure in the Gulf of Alaska. *Limnology and Oceanography*, *56*(3), 1023–1034. https://doi.org/10.4319/lo.2011.56.3.1023

Kolber, Z. S., Prasil, O., & Falkowski, P. G. (1998). Measurements of variable chlorophyll fluorescence using fast repetition rate techniques: Defining methodology and experimental protocols. *Biochimica et Biophysica Acta - Bioenergetics*, *1367*(1–3), 88–106. https://doi.org/10.1016/S0005-2728(98)00135-2

Liu, X., & Millero, F. J. (2002). The solubility of iron in seawater. *Marine Chemistry*, *77*(1), 43–54. https://doi.org/10.1016/S0304-4203(01)00074-3

Lohan, M. C., & Bruland, K. W. (2008). Elevated Fe (II) and dissolved Fe in hypoxic shelf waters off Oregon and Washington: An enhanced source of iron to coastal upwelling regimes. *Environmental Science & Technology*, *42*(17), 6462–6468. https://doi.org/10.1021/es800144j

Macey, A. I., Ryan-Keogh, T., Richier, S., Moore, C. M., & Bibby, T. S. (2014). Photosynthetic protein stoichiometry and photophysiology in the high latitude North Atlantic. *Limnology and Oceanography*, *59*(6), 1853–1864. https://doi.org/10.4319/lo.2014.59.6.1853

Mackas, D. L., Denman, K. L., & Abbott, M. R. (1985). Plankton patchiness: Biology in the physical vernacular. *Bulletin of Marine Science*, *37*(2), 653–674.

Martin, J. H., Coale, K. H., Johnson, K. S., Fitzwater, S. E., Gordon, R. M., Tanner, S. J., et al. (1994). Testing the iron hypothesis in ecosystems of the equatorial Pacific Ocean. *Nature*, *371*(6493), 123–129. https://doi.org/10.1038/371123a0

Martinez, S., Yang, X., Bennett, B., & Holz, R. C. (2017). A cobalt-containing eukaryotic nitrile hydratase. *Biochimica et Biophysica Acta (BBA)-Proteins and Proteomics*, *1865*(1), 107–112. https://doi.org/10.1016/j.bbapap.2016.09.013

Moore, C. M., Mills, M. M., Arrigo, K. R., Berman-Frank, I., Bopp, L., Boyd, P. W., et al. (2013). Processes and patterns of oceanic nutrient limitation. *Nature Geoscience*, *6*(9), 701–710. https://doi.org/10.1038/ngeo1765

Moore, C. M., Mills, M. M., Milne, A., Langlois, R., Achterberg, E. P., Lochte, K., et al. (2006). Iron limits primary productivity during spring bloom development in the Central North Atlantic. *Global Change Biology*, *12*(4), 626–634. https://doi.org/10.1111/j.1365-2486.2006.01122.x

Morel, F. M. M., Milligan, A. J., & Saito, M. A. (2003). Marine bioinorganic chemistry: The role of trace of metals in the oceanic cycles of major nutrients. In H. D. Holland, & K. K. Turekian (Eds.), *The oceans and marine geochemistry*, *Treatise on Geochemistry* (Vol. 6, pp. 113–143). Cambridge: Elsevier.

Noble, A. E., Lamborg, C. H., Ohnemus, D. C., Lam, P. J., Goepfert, T. J., Measures, C. I., et al. (2012). Basin-scale inputs of cobalt, iron, and manganese from the Benguela-Angola front to the South Atlantic Ocean. *Limnology and Oceanography*, *57*(4), 989–1010. https://doi.org/10.4319/lo.2012.57.4.0989

Panzeca, C., Beck, A. J., Leblanc, K., Taylor, G. T., Hutchins, D. A., & Sañudo-Wilhelmy, S. A. (2008). Potential cobalt limitation of vitamin B12 synthesis in the North Atlantic Ocean. *Global Biogeochemical Cycles*, *22*, GB2029. https://doi.org/10.1029/2007GB003124

Parekh, P., Follows, M. J., & Boyle, E. A. (2005). Decoupling of iron and phosphate in the global ocean. *Global Biogeochemical Cycles*, *19*, GB2020. https://doi.org/10.1029/2004GB002280

Price, N. M., Harrison, G. I., Hering, J. G., Hudson, R. J., Nirel, P. M., Palenik, B., & Morel, F. M. (1989). Preparation and chemistry of the artificial algal culture medium Aquil. *Biological Oceanography*, *6*(5–6), 443–461.

Rapp, I., Schlosser, C., Rusiecka, D., Gledhill, M., & Achterberg, E. P. (2017). Automated preconcentration of Fe, Zn, Cu, Ni, Cd, Pb, Co, and Mn in seawater with analysis using high-resolution sector field inductively-coupled plasma mass spectrometry. *Analytica Chimica Acta*, *976*, 1–13. https://doi.org/10.1016/j.aca.2017.05.008

Resing, J. A., Sedwick, P. N., German, C. R., Jenkins, W. J., Moffett, J. W., Sohst, B. M., & Tagliabue, A. (2015). Basin-scale transport of hydrothermal dissolved metals across the South Pacific Ocean. *Nature*, *523*(7559), 200–203. https://doi.org/10.1038/nature14577

Ryan-Keogh, T. J., Macey, A. I., Nielsdóttir, M. C., Lucas, M. I., Steigenberger, S. S., Stinchcombe, M. C., et al. (2013). Spatial and temporal development of phytoplankton iron stress in relation to bloom dynamics in the high-latitude North Atlantic Ocean. *Limnology and Oceanography*, *58*(2), 533–545. https://doi.org/10.4319/lo.2013.58.2.0533

Saito, M. A., Goepfert, T. J., & Ritt, J. T. (2008). Some thoughts on the concept of colimitation: Three definitions and the importance of bioavailability. *Limnology and Oceanography*, *53*(1), 276–290. https://doi.org/10.4319/lo.2008.53.1.0276

Saito, M. A., McIlvin, M. R., Moran, D. M., Goepfert, T. J., DiTullio, G. R., Post, A. F., & Lamborg, C. H. (2014). Multiple nutrient stresses at intersecting Pacific Ocean biomes detected by protein biomarkers. *Science*, *345*(6201), 1173–1177. https://doi.org/10.1126/science.1256450

Saito, M. A., Moffett, J. W., & DiTullio, G. R. (2004). Cobalt and nickel in the Peru upwelling region: A major flux of labile cobalt utilized as a micronutrient. *Global Biogeochemical Cycles*, *18*, GB4030. https://doi.org/10.1029/2003GB002216

Saito, M. A., Noble, A. E., Hawco, N., Twining, B. S., Ohnemus, D. C., John, S. G., et al. (2017). The acceleration of dissolved cobalt's ecological stoichiometry due to biological uptake, remineralization, and scavenging in the Atlantic Ocean. *Biogeosciences*, *14*(20), 4637–4662. https://doi.org/10.5194/bg-14-4637-2017

Saito, M. A., Rocap, G., & Moffett, J. W. (2005). Production of cobalt binding ligands in a Synechococcus feature at the Costa Rica upwelling dome. *Limnology and Oceanography*, *50*(1), 279–290. https://doi.org/10.4319/lo.2005.50.1.0279

Sañudo-Wilhelmy, S. A., Cutter, L. S., Durazo, R., Smail, E. A., Gómez-Consarnau, L., Webb, E. A., et al. (2012). Multiple B-vitamin depletion in large areas of the coastal ocean. *Proceedings of the National Academy of Sciences of the United States of America*, *109*(35), 14,041–14,045. https://doi.org/10.1073/pnas.1208755109

Schlosser, C., De La Roche, C. L., Streu, P., & Croot, P. L. (2012). Solubility of iron in the Southern Ocean. *Limnology and Oceanography*, *57*(3), 684–697. https://doi.org/10.4319/lo.2012.57.3.0684

Scholz, F., Löscher, C. R., Fiskal, A., Sommer, S., Hensen, C., Lomnitz, U., et al. (2016). Nitrate-dependent iron oxidation limits iron transport in anoxic ocean regions. *Earth and Planetary Science Letters*, *454*, 272–281. https://doi.org/10.1016/j.epsl.2016.09.025

Shaked, Y., & Lis, H. (2012). Disassembling iron availability to phytoplankton. *Frontiers in Microbiology*, *3*, 1–26. https://doi.org/10.3389/fmicb.2012.00123

Sperfeld, E., Raubenheimer, D., & Wacker, A. (2016). Bridging factorial and gradient concepts of resource co-limitation: Towards a general framework applied to consumers. *Ecology Letters*, *19*(2), 201–215. https://doi.org/10.1111/ele.12554

Stramma, L., Fischer, T., Grundle, D. S., Krahmann, G., Bange, H. W., & Marandino, C. A. (2016). Observed El Nino conditions in the eastern tropical Pacific in October 2015. *Ocean Science*, *12*(4), 861–873. https://doi.org/10.5194/os-12-861-2016

Tagliabue, A., Mtshali, T., Aumont, O., Bowie, A. R., Klunder, M. B., Roychoudhury, A. N., & Swart, S. (2012). A global compilation of dissolved iron measurements: Focus on distributions and processes in the Southern Ocean. *Biogeosciences*, *9*(6), 2333–2349. https://doi.org/10.5194/bg-9-2333-2012

Taylor, B. B., Torrecilla, E., Bernhardt, A., Taylor, M. H., Peeken, I., Röttgers, R., et al. (2011). Bio-optical provinces in the eastern Atlantic Ocean and their biogeographical relevance. *Biogeosciences*, *8*(12), 3609–3629. https://doi.org/10.5194/bg-8-3609-2011

Ulloa, O., Escribano, R., Hormazabal, S., Quinones, R. A., González, R. R., & Ramos, M. (2001). Evolution and biological effects of the 1997–98 El Nino in the upwelling ecosystem off northern Chile. *Geophysical Research Letters*, *28*(8), 1591–1594. https://doi.org/10.1029/2000GL011548

Welschmeyer, N. A. (1994). Fluorometric analysis of chlorophyll a in the presence of chlorophyll b and pheopigments. *Limnology and Oceanography*, *39*(8), 1985–1992. https://doi.org/10.4319/lo.1994.39.8.1985

Yee, D., & Morel, F. M. M. (1996). In vivo substitution in carbonic of zinc by cobalt of a marine anhydrase diatom. *Limnology and Oceanography*, *41*(3), 573–577.